

Cooling of a Zero-Nuclear-Spin Molecular Ion to a Selected Rotational State

Patrick R. Stollenwerk,^{1,*} Ivan O. Antonov,^{1,*} Sruthi Venkataramanababu,² Yen-Wei Lin,¹ and Brian C. Odom^{1,†}

¹*Department of Physics and Astronomy, Northwestern University, Evanston, Illinois 60208, USA*

²*Graduate Program in Applied Physics, Northwestern University, Evanston, Illinois 60208, USA*

(Dated: June 16, 2022)

We demonstrate rotational cooling of the silicon monoxide cation via optical pumping by a spectrally filtered broadband laser. Compared with diatomic hydrides, SiO^+ is more challenging to cool because of its smaller rotational interval. However, the rotational level spacing and large dipole moment of SiO^+ allows direct manipulation by microwaves, and the absence of hyperfine structure in its dominant isotopologue greatly reduces demands for pure quantum state preparation. These features make $^{28}\text{Si}^{16}\text{O}^+$ a good candidate for future applications such as quantum information processing. Cooling to the ground rotational state is achieved on a 100 ms time scale and attains a population of 94(3)%, with an equivalent temperature $T = 0.53(6)$ K. We also describe a novel spectral-filtering approach to cool into arbitrary rotational states and use it to demonstrate a narrow rotational population distribution ($\Delta N = 2$) around a selected state.

INTRODUCTION

A broad range of physics and chemistry interest motivates developing tools for robust control over molecular internal degrees of freedom. Applications include study of cold collisions [1, 2], quantum state-dependent chemistry [3–5], astrochemistry [6], many-body physics [7–10], and quantum information processing [11, 12]. Tests of fundamental physics using precision spectroscopy of molecules also require quantum state preparation [13]. Molecules, in contrast to free atoms, have rotational and vibrational degrees of freedom via their chemical bonds. On one hand, these extra degrees of freedom extend the scope of possible control and provide the rich structure that generates their appeal. On the other hand, their level structure can be quite complicated and thus challenging for state control since phase space grows exponentially with the number of degrees of freedom. Despite this increased complexity, substantial progress on state preparation of molecules has been made in the past decade using several techniques including optical pumping [14–18], buffer-gas cooling [19, 20], state-selective photoionization [21], projective preparation of a pure quantum state using quantum logic [22], supersonic expansion of molecular beams [23], and photoassociation [24].

Trapped molecular ions in Coulomb crystals can be isolated from environmental influence and are particularly well-suited for precision spectroscopy, quantum information processing, and other applications requiring uninterrupted dynamics over long time scales. State preparation by optical pumping allows rapid and repetitive resetting of the molecular state, often desired in these applications. Optical pumping of trapped molecular ion rotations has previously been demonstrated for diatomic hydrides [15, 16, 18]. However, the non-zero nuclear spin of hydrogen (or deuterium) couples with the rotational degree of freedom and any non-zero nuclear spin of the other atom, making high-fidelity optical pumping to a pure internal state still a challenge [25]. In contrast, di-

atomic molecules with two $I = 0$ species have no complicating hyperfine structure. Furthermore, oxides and other molecules with heavier reduced masses have smaller rotational spacing than do hydrides (43 GHz for lowest the lowest SiO^+ rotational interval). SiO^+ is a polar molecule with a sizeable body-frame dipole moment of 4.1 – 4.4 Debye [26–29], so transitions between adjacent rotational states can be coherently driven with convenient microwave sources.

Even for the simplest molecules, coupling of electronic and vibrational motion usually precludes cycling on an electronic transition without lasers to repump incidental vibrational excitations. Several groups have noted the advantage of optical pumping with the class of molecules whose ground and excited electronic states have nearly identical bond equilibrium distances, i.e. molecules with nearly diagonal Franck-Condon Factors (FCFs) [30–33] such as AlH^+ and SiO^+ . The strong overlap in vibrational wavefunctions decouples vibrational excitation from electronic relaxation and thus accommodates repetitive pumping with a small number of lasers. Broadband lasers with relatively simple spectral filtering have been used to achieve high-fidelity cooling to the ground rotational state of AlH^+ [18]. Since the rotational constant of SiO^+ is nearly an order of magnitude smaller, rotational cooling of this new species to a similar degree requires significantly better spectral filtering. Filtered broadband lasers have also been used to obtain significant vibrational and rotational cooling of BaF [17].

In this Letter we demonstrate ground state rotational cooling of trapped $^{28}\text{Si}^{16}\text{O}^+$ to a ground state population of 0.94(3) corresponding to a temperature of 0.53(6)K. We also propose and demonstrate a spectral filtering scheme for preparing arbitrary target rotational states of SiO^+ . We develop a simplified analytic model to characterize the time scales for state preparation.

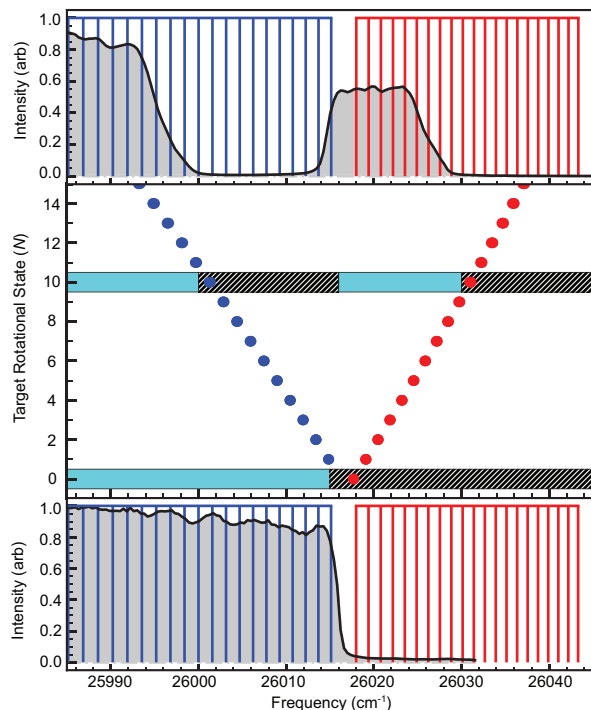


FIG. 1. **(Center)** Spectral masks overlaid onto the Fortrat diagram of the $\text{SiO}^+ B - X(0,0)$ transition. P and R -branch transitions are indicated by blue and red dots respectively. The blocked spectrum for each mask is indicated by the dark hashes. The measured optical pumping spectra which have been filtered to target the ground rotational state **(Bottom)** and $N = 10$ **(Top)** are shown with the relevant P and R -branch transitions indicated by blue and red vertical lines.

SPECTRAL FILTERING

State preparation of SiO^+ was achieved by spectrally filtering a frequency doubled Spectra-Physics MaiTai HP laser tuned to the $B^2\Sigma^+ - X^2\Sigma^+$ electronic transition near 385 nm. Spectral filtering is done by using the $2 - f$ configuration of the pulse-shaping setup described in [34]. The $B - X$ transition was chosen because the electronic resonance is weakly coupled to vibrations (diagonal FCFs), allowing on average more than 30 optical pumping cycles before the vibrational quantum number changes [35]. Diagonal FCFs also imply the states have nearly identical rotational constants resulting in a spectrum well separated according to angular momentum selection rules.

For ground state preparation the spectral filtering mask requires pumping of only the P -branch transitions ($\Delta N = -1$) which is accomplished by blocking the high frequency components at the Fourier plane with a razor blade (Fig. 1) [18, 36]. To extend preparation to arbitrary $N > 0$ rotational states, a mask on the P -branch must be introduced to only pump down to the target state, and the mask on the R -branch needs to be shifted to allow pumping up to the target state. This is accomplished

with the removal of a band in the middle of the spectrum in addition to the removal of the high frequency components. This band is filtered using a thin ($25 \mu\text{m}$) metal ribbon whose profile is adjusted by rotating to match the required bandwidth at the Fourier plane (Fig. 1). In this way, each rotational level is exclusively pumped toward higher or lower N , with exception of the target state which is intentionally left dark.

TRAPPING AND DETECTION

Quantum state control experiments were performed at room temperature under ultra-high vacuum conditions ($7(4) \times 10^{-10}$ Torr). For each data point a sample of 10 to 100 SiO^+ was co-loaded with 500 to 1000 laser cooled barium ions in a linear Paul trap. Loading of SiO^+ was performed using the $\text{SiO } A^1\Pi - X^1\Sigma^+(5,0)$ 1+1 REMPI transition following ablation of a solid SiO sample [37]. Translational energy is rapidly cooled sympathetically by Ba^+ , however molecular internal degrees of freedom are decoupled from translational motion. The interval between loading and data collection is typically 30 s. SiO^+ is expected to be loaded between $N = 4$ and $N = 15$ [37]. Consistent with this and the measured slow thermalization out of $N = 0$ (Fig. 3), we do not observe significant population in $N = 0$ without application of the cooling laser.

The trapped SiO^+ were detected using an in-situ laser cooled fluorescence mass spectrometry (LCFMS) [38] technique. Briefly, the radial secular motion of the SiO^+ was resonantly excited using a low amplitude (0.5-1 V) RF waveform applied to one of the radial trapping rods. This resulted in Doppler broadening of the Ba^+ resonance and a decrease of Ba^+ fluorescence in proportion to the number of SiO^+ in the trap.

State detection of SiO^+ was performed destructively using single-photon resonance-enhanced photodissociation spectroscopy via the predissociative $C^2\Pi$ state, which has a lifetime sufficiently long to achieve rotational resolution and sufficiently short for efficient dissociation. The state was previously reported in theoretical studies as the $2^2\Pi$ state [27–29, 39, 40]. It had not been observed experimentally prior to this work. A manuscript detailing spectroscopy of the $C^2\Pi$ state is currently in preparation [41].

A pulsed dye laser with output near 226 nm is used for dissociation. Predissociation of SiO^+ via the $C^2\Pi$ state leads to the $\text{Si}^+ + \text{O}$ product channel. In the work described here we monitored the SiO^+ signal to measure the dissociated fraction. We performed two types of measurements to characterize state control.

The first method is based on a slow steady-state depletion, where the depletion rate constant yields the state population. The LCFMS SiO^+ signal was monitored while simultaneously firing the dissociation laser at 10

Hz onto the sample for a total of 300 pulses. The signal was fit to an exponential decay to obtain a rate R . The fraction of molecules d dissociated per pulse is given by

$$d = pn \approx 1 - e^{-R/(10 \text{ Hz})} \approx R/(10 \text{ Hz}) \quad (1)$$

where p is the probability per pulse of dissociating a molecule from the target state, and n is the fractional population in that state. To ensure that the approximations in Eqn. (1) are valid and that steady-state is achieved before each dissociation pulse, we require $p \ll 1$, $R/(2\pi) \ll 10 \text{ Hz}$, and $R \ll \Gamma$, where Γ is the equilibration rate of the probed state. Experimentally, we reduce the dissociation laser fluence until these conditions are met, and it can be verified that inferred populations are independent of the fluence. R is plotted as a function of dissociation laser wavelength to obtain a spectrum.

This method yields only relative populations, but has advantages for the signal-to-noise ratio (SNR) and dynamic range. All the molecules in the sample contribute toward the statistics, even for probed states with relatively low populations. Factoring out unknown constants such as the electronic and vibrational transition moments (which remain constant over the rotational manifold) and laser fluence, relative spectra can be taken with approximately constant SNR over an R dynamic range of more than two orders of magnitude provided the laser fluence is low enough.

The second method is a single-shot depletion technique [15, 16, 36]. To detect the absolute population fraction, we recorded the LCFMS signal before and after a single intense pulse. Because the predissociation lifetime of the upper state is shorter than the pulse duration, 100% dissociation probability is achievable. This method probes absolute state populations but lacks the advantages of the steady-state method discussed above.

RELATIVE COOLING EFFICIENCY

Fig. 2(a) shows the $|X^2\Sigma^+, v=0\rangle \rightarrow |C^2\Pi_{3/2}, v=1\rangle$ spectrum after the population has been pumped towards the $N=0$ state. This vibronic transition to the upper spin-orbit state was chosen because the shifted lines from other isotopologues are well separated from the sampled range, and there is only one line originating from $N=0$ which is well separated from $N=1$ lines. In Fig. 2, we use the notation $x(N)$ to denote the lines, where x represents the branch type characterized by $\Delta N = (J'+1/2) - N$, and N is the originating rotational state, e.g. ${}^sR_{21}(0.5)$ is denoted $s(0)$. We simulated the spectrum using PGOPHER [42] and fit the spectral envelope to obtain a ratio of population in $N=1$ to $N=0$ of 0.075(3) (Fig. 2(c)). We also demonstrate cooling into an excited rotational state (Fig. 2(b)) by applying the spectral mask for $N=10$ (Fig. 1). Both the $N=0$ and

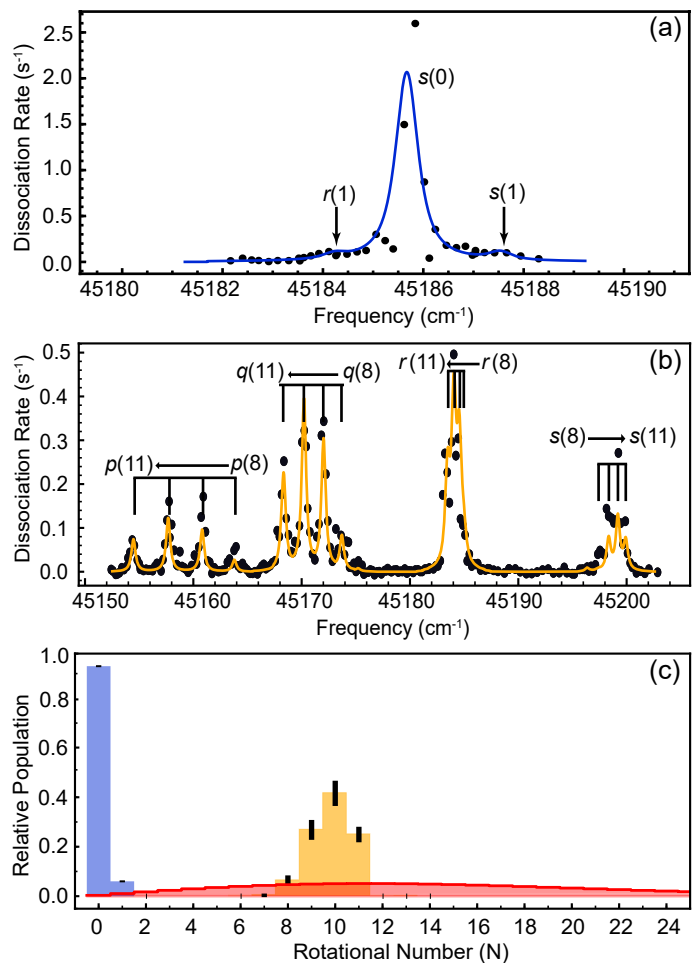


FIG. 2. The $X^2\Sigma^+ \rightarrow C^2\Pi_{3/2}(1,0)$ dissociation spectrum of SiO^+ optically pumped (a) towards $N=0$ and (b) $N=10$. (c) Relative rotational state populations inferred from the dissociation spectra and their $\pm 1\sigma$ uncertainties, along with a 300 K thermal distribution.

$N=10$ spectra are in sharp contrast with a thermal distribution at 300 K.

Although the steady-state analysis technique does not directly yield absolute populations, some qualitative conclusions can be drawn about possible populations in other states. Scans searching for transitions originating from $v=1$ did not show any discernable peaks. Furthermore, the states in the low-lying $A^2\Pi$ manifold are too short-lived for significant population accumulation. A quantitative measurement setting bounds on these populations is discussed in the section below.

ABSOLUTE COOLING EFFICIENCY AND TIMESCALE

Fig. 3 shows the measured population accumulation in $N=0$ when pumping toward that state, ana-

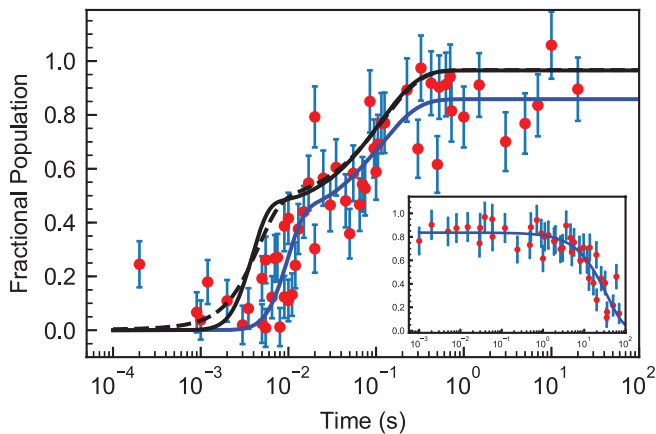


FIG. 3. Single-shot analysis of $N = 0$ population versus optical pumping time. Solid lines are fits to the simulation (dashed line) and uncorrected raw data. (Inset) Measured longevity of $N = 0$ state after the sample was prepared by optical pumping.

lyzed using the single-shot method. Here, we used the $|X^2\Sigma^+, v = 0, N = 0\rangle \rightarrow |C^2\Pi_{1/2}, v = 0, J = 0.5\rangle$ transition at 44044.5 cm^{-1} . The anomalous point at very short times is understood to be a spurious signal from population in $N = 11$, which has an overlapping line.

Two time scales are present. The faster time scale is for cooling of the separate parity populations independently. Optical cycling on the diagonal $B - X$ transitions is a parity-preserving process and thus approximately half of the population is unable to be directly pumped into the even parity ground rotational state. For population beginning in an even parity state, optical pumping down the rotational ladder can be modeled by a rate λ for population transfer from N to $N - 2$, where λ varies by less than a factor of 2 across the P -branch [43]. Neglecting this weak dependence, we arrive at a simple analytic expression for pumping of population initially in $N = 2M$ into $N = 0$:

$$n_0(t) = 1 - e^{-\lambda t} \sum_{i=0}^{M-1} \frac{(\lambda t)^i}{i!}. \quad (2)$$

The slower time scale is determined by the rate of parity flips. The details of this process have not been determined, but it likely starts from population cooled to the lowest negative parity state ($N = 1$) being continuously driven on the quasi-cycling $P(1)$ transition, until it leaks elsewhere. The required odd number of electric-dipole transitions could occur in decay channels passing through intermediate $|X, v > 0\rangle$ or $|A\rangle$ states. Off-diagonal decay from $|B, v = 0\rangle \rightarrow |X, v > 0\rangle$ has a reasonable branching ratio, but subsequent $|X, v > 0\rangle$ vibrational relaxation is much longer than the observed timescale. Likewise, although the predicted lifetime of $|A\rangle$ is itself short enough, decay from $|B, v = 0\rangle \rightarrow |A\rangle$ is predicted to have too small a branching ratio [29]. However, a hybrid mech-

TABLE I. Absolute cooling efficiency fitted parameters, systematic shifts, and results.

Cooling Rate Parameters		Systematic Effects	
	Data	Sim.	ΔA Unc.
$\lambda \text{ (s}^{-1}\text{)}$	650(90)	1630	Isotope -0.07 < 0.002
			Reaction -0.038 0.010
$\lambda_P \text{ (s}^{-1}\text{)}$	9(4)	8.9	n_1 +0.006 < 0.005
			Total ΔA $\overline{-0.102}$ $\overline{0.011}$
Absolute Cooling Efficiency			
n_0^a	0.94(3)	$n_{0,sim}$	0.97
$T \text{ (K)}$	0.53(6)	$T_{sim} \text{ (K)}$	0.47

^a Asymptotic $N = 0$ population using $n_0 = A - \Delta A$, where A is the asymptotic value from the fits.

anism seems plausible. Population in $|X, v = 2\rangle$ would continue to be driven to $|B, v = 2\rangle$ by the cooling laser and eventually undergo a decay $|B, v = 2\rangle \rightarrow |A, v = 0\rangle$, which has an enhanced rate due to a near degeneracy and resultant strong coupling between the states [44]. Regardless of the parity flip mechanism, by modeling the process as governed by a rate λ_P , population transfer from $N = 2M + 1$ to $N = 0$ is analytically found to be

$$n_0(t) = 1 - e^{-\lambda t} \left(\sum_{i=0}^M \frac{(\lambda t)^i}{i!} + \sum_{i=M+1}^{\infty} \frac{(\lambda - \lambda_P)^i t^i}{i!(1 - \lambda_P/\lambda)^M} \right). \quad (3)$$

For slow parity exchange $\lambda_P \ll \lambda/M$, the result asymptotically approaches $1 - e^{-\lambda_P t}$.

The cooling data are fit to a sum of Eqns. (2) and (3), with the results shown in Fig. 3 and Table I. The initial distribution is expected to peak around $N = 12$ [37], so $M = 6$ is used in the fitting function. The asymptotic limit of the fits in Fig. 3 and inset are used to determine the fidelity of ground state preparation and an equivalent temperature. Also shown are the results of an Einstein rate equation simulation [45] using the experimental spectral intensity and spectral cutoff sharpness of the cooling laser, with SiO^+ initialized to a 300 K distribution. Systematic shifts, which predict an offset between raw data and the simulation, include reaction with the background hydrogen, impure isotope selection, and partial spectral overlap of the laser linewidth with other dissociating transitions. SiO^+ reacts with background H_2 [46], so the maximum possible dissociation fraction of SiO^+ is reduced from 1. The most abundant isotopologue is $^{28}\text{Si}^{16}\text{O}$ with a natural abundance of 92%. The shifts of $^{29}\text{Si}^{16}\text{O}^+$ and $^{30}\text{Si}^{16}\text{O}^+$ are expected to be 0.51 cm^{-1} and 0.99 cm^{-1} respectively; thus, probability of their dissociation is reduced. Transitions originating from $N = 1$ are roughly one linewidth away and also contribute to the dissociated fraction. The details of these systematics are discussed in [43]. Accounting for the sys-

tematic effects, we conclude that the steady-state $N = 0$ absolute population fraction of the dominant isotope is 0.94(3), which corresponds to a temperature of 0.53(6) K. This result is in agreement with both the simulation and the relative population analysis.

Thermalization of SiO^+ out of $N = 0$, after the cessation of optical pumping, is shown in the inset of Fig. 3. The population loss is well fit by an exponential decay with a time constant of 35(4) s. This time scale is much faster than blackbody-induced pure rotational or vibrational excitations, and also faster than the observed reaction rate with H_2 of ~ 10 minutes. However, it could be consistent with inelastic collisions with H_2 , which have a Langevin collision time of 40(20) s, with uncertainty coming from the H_2 pressure. Blackbody redistribution via the A state is also a possible mechanism, expected to occur on a time scale of 70 - 130 s given predicted A state lifetimes of a few milliseconds [29, 32].

CONCLUSIONS

This work demonstrates the extension of a broadband rotational cooling technique from diatomic hydrides to the oxides; the latter being more challenging because of a smaller rotational splitting for optical pumping. Furthermore, we show that the class of diagonal molecules amenable to rotational cooling can be extended to include those with an intermediate electronic state not involved in the dominant optical cycling. Zero nuclear spin molecules such as $^{28}\text{Si}^{16}\text{O}^+$ are good candidates for applications that require preparation of a pure quantum state, such as quantum information processing and single-molecule precision spectroscopy.

Higher resolution spectral filtering is possible, for example by using a virtual imaged phased array (VIPA) where sub-GHz pulse shaping resolution has been achieved [47]. This technique could significantly enhance the preparation fidelity of the $N = 0$ and $N = 10$ states shown here. Consequently, it might be advantageous to use $N > 0$ states for quantum information processing, since dominant decoherence mechanisms are reduced for higher rotational states [11]. $N > 0$ preparation is also useful for spectroscopic studies and can provide insights into the molecular Hamiltonian at high energies [41].

The limiting timescale is currently the parity cooling step. The electronic decay from A to X is predicted to be of order 5 ms, thus we expect that the cooling rate could be increased by more than an order of magnitude with increased spectral fluence of the pump laser. An alternative would be to use microwaves to drive parity flips, for instance at 86 GHz connecting $N = 1$ with $N = 2$ [48] for cooling to $N = 0$. Use of a microwave drive could equalize the timescales for cooling the two parities, and with a more intense cooling laser $^{28}\text{Si}^{16}\text{O}^+$ population could be cooled to a pure internal quantum state in $< 10 \mu\text{s}$,

limited by the spontaneous emission rate of B . Further refinements may enable efficient fluorescent imaging or direct Doppler cooling of SiO^+ [29, 32]. Such improvements could help realize multi-ion molecular clocks with canceling Stark and second order Doppler shifts [45].

It is interesting to consider optical pumping on arbitrary molecules. Use of VIPA could directly extend the technique discussed here to diagonal-FCF molecules of heavier reduced mass. The development of broadband and spectrally bright supercontinuum lasers may eventually allow efficient optical pumping of non-diagonal molecules with a very small number of repump lasers. Furthermore, replacing the spectral mask with a digital micro-mirror array [49] will allow for construction of more complex masks which can vary in time, potentially guiding population through spectrally congested regions with conflicting selection rules [41].

However, it is important to recognize the value of a control technique does not rest exclusively on its generality. Our demonstration of optical pumping of $^{28}\text{Si}^{16}\text{O}^+$ to a well-defined internal state suggests this species could play a similar role in a wide range of molecular applications, as do only a relatively small handful of popular atomic species.

We gratefully acknowledge Jason Nguyen for proposing rotational cooling of SiO^+ , along with his and David Tabor's early work on SiO^+ in the lab. Development of dissociative analysis techniques were funded by NSF Grant No. PHY-1806861, LCFMS techniques were funded by ARO Grant No. W911NF-14-0378, and optical state control techniques were funded by AFOSR Grant No. FA9550-17-1-0352.

* Equally contributing authors

† b-odom@northwestern.edu

- [1] D. Zhang and S. Willitsch, in *Cold Chemistry* (2017), pp. 496–536.
- [2] A. D. Dörfler, P. Eberle, D. Koner, M. Tomza, M. Meuwly, and S. Willitsch, *Nat. Commun.* **10**, 1 (2019).
- [3] M. T. Bell and T. P. Softley, *Mol. Phys.* **107**, 99 (2009).
- [4] J. M. Hutson, *Science* **327**, 788 (2010).
- [5] N. Balakrishnan, *J. Chem. Phys.* **145**, 150901 (2016).
- [6] W. S. Ian, *Low temperatures and cold molecules* (World Scientific, 2008).
- [7] B. Yan, S. A. Moses, B. Gadway, J. P. Covey, K. R. Hazzard, A. M. Rey, D. S. Jin, and J. Ye, *Nature* **501**, 521 (2013).
- [8] K. R. A. Hazzard, B. Gadway, M. Foss-Feig, B. Yan, S. A. Moses, J. P. Covey, N. Y. Yao, M. D. Lukin, J. Ye, D. S. Jin, A. M. Rey, *Phys. Rev. Lett.* **113**, 195302 (2014).
- [9] R. Schmidt and M. Lemesko, *Phys. Rev. Lett.* **114**, 203001 (2015).
- [10] R. Schmidt and M. Lemesko, *Phys. Rev. X* **6**, 011012 (2016).
- [11] E. R. Hudson and W. C. Campbell, *Phys. Rev. A* **98**,

- 040302(R) (2018).
- [12] W. C. Campbell and E. R. Hudson, arXiv preprint [arXiv:1909.02668](https://arxiv.org/abs/1909.02668) (2019).
- [13] M. S. Safronova, D. Budker, D. DeMille, D. F. J. Kimball, A. Derevianko, and C. W. Clark, *Rev. Mod. Phys.* **90**, 025008 (2018).
- [14] M. Viteau, A. Chotia, M. Allegrini, N. Bouloufa, O. Dulieu, D. Comparat, and P. Pillet, *Science* **321**, 232 (2008).
- [15] P. F. Staantum, K. Højbjerg, P. S. Skyt, A. K. Hansen, and M. Drewsen, *Nat. Phys.* **6**, 271 (2010).
- [16] T. Schneider, B. Roth, H. Duncker, I. Ernsting, and S. Schiller, *Nat. Phys.* **6**, 275 (2010).
- [17] A. Cournol, P. Pillet, H. Lignier, and D. Comparat, *Phys. Rev. A* **97**, 031401(R) (2018).
- [18] C.-Y. Lien, C. M. Seck, Y.-W. Lin, J. H. Nguyen, D. A. Tabor, and B. C. Odom, *Nat. Commun.* **5**, 4783 (2014).
- [19] W. G. Rellergert, S. T. Sullivan, S. J. Schowalter, S. Kotochigova, K. Chen, and E. R. Hudson, *Nature* **495**, 490 (2013), ISSN 1476-4687.
- [20] A. K. Hansen, O. Versolato, S. B. Kristensen, A. Ginggell, M. Schwarz, A. Windberger, J. Ullrich, J. C. López-Urrutia, M. Drewsen, et al., *Nature* **508**, 76 (2014).
- [21] X. Tong, A. H. Winney, and S. Willitsch, *Phys. Rev. Lett.* **105**, 143001 (2010).
- [22] C.-w. Chou, C. Kurz, D. B. Hume, P. N. Plessow, D. R. Leibbrandt, and D. Leibfried, *Nature* **545**, 203 (2017).
- [23] Y. Shagam and E. Narevicius, *The Journal of Physical Chemistry C* **117**, 22454 (2013).
- [24] K.-K. Ni, S. Ospelkaus, M. De Miranda, A. Pe'Er, B. Neyenhuis, J. Zirbel, S. Kotochigova, P. Julienne, D. Jin, and J. Ye, *Science* **322**, 231 (2008).
- [25] U. Bressel, A. Borodin, J. Shen, M. Hansen, I. Ernsting, and S. Schiller, *Phys. Rev. Lett.* **108**, 183003 (2012).
- [26] H.-J. Werner, P. Rosmus, and M. Grimm, *Chem. Phys.* **73**, 169 (1982).
- [27] Z.-L. Cai and J.-P. François, *J. Mol. Spectrosc.* **197**, 12 (1999).
- [28] S. Chattopadhyaya, A. Chattopadhyay, and K. K. Das, *J. Mol. Struct. THEOCHEM* **639**, 177 (2003).
- [29] R. Li, X. Yuan, G. Liang, Y. Wu, J. Wang, and B. Yan, *Chem. Phys.* **525**, 110412 (2019).
- [30] M. D. Di Rosa, *Eur. Phys. J. D* **31**, 395 (2004), ISSN 1434-6079.
- [31] D. Sofikitis, S. Weber, A. Fioretti, R. Horchani, M. Allegrini, B. Chatel, D. Comparat, and P. Pillet, *New J. Phys.* **11**, 055037 (2009).
- [32] J. H. V. Nguyen and B. Odom, *Phys. Rev. A* **83**, 053404 (2011).
- [33] J. H. V. Nguyen, C. R. Viteri, E. G. Hohenstein, C. D. Sherrill, K. R. Brown, and B. Odom, *New J. Phys.* **13**, 063023 (2011).
- [34] Y.-W. Lin and B. C. Odom, arXiv:1610.04324 (2016).
- [35] P. R. Stollenwerk, B. C. Odom, D. L. Kokkin, and T. Steimle, *J. Mol. Spectrosc.* **332**, 26 (2017).
- [36] C.-Y. Lien, S. R. Williams, and B. Odom, *Phys. Chem. Chem. Phys.* **13**, 18825 (2011).
- [37] P. R. Stollenwerk, I. O. Antonov, and B. C. Odom, *J. Mol. Spectrosc.* **355**, 40 (2019).
- [38] T. Baba and I. Waki, *J. Appl. Phys.* **89**, 4592 (2001).
- [39] N. Honjou, *Mol. Phys.* **101**, 3063 (2003).
- [40] D. Shi, W. Li, W. Xing, J. Sun, Z. Zhu, and Y. Liu, *Comput. Theor. Chem.* **980**, 73 (2012).
- [41] (manuscript in preparation).
- [42] C. M. Western, *J. Quant. Spectrosc. Radiat. Transfer* **186**, 221 (2017).
- [43] P. R. Stollenwerk, Ph.D. thesis, Department of Physics Northwestern University (2020).
- [44] S. D. Rosner, R. Cameron, T. J. Scholl, and R. A. Holt, *J. Mol. Spectrosc.* **189**, 83 (1998).
- [45] P. R. Stollenwerk, M. G. Kokish, A. G. S. de Oliveira-Filho, F. R. Ornellas, and B. C. Odom, *Atoms* **6**, 53 (2018).
- [46] D. Fahey, F. Fehsenfeld, E. Ferguson, and L. Viehland, *J. Chem. Phys.* **75**, 669 (1981).
- [47] J. T. Willits, A. M. Weiner, and S. T. Cundiff, *Opt. Express* **20**, 3110 (2012).
- [48] T. J. Scholl, R. Cameron, S. D. Rosner, and R. A. Holt, *Can. J. Phys.* **73**, 101 (1995).
- [49] R. Horchani, *Opt. Quantum. Electron.* **47**, 3023 (2015).